

## Review Article

## Neurosurgical confocal endomicroscopy: A review of contrast agents, confocal systems, and future imaging modalities

Aqib H. Zehri<sup>1</sup>, Wyatt Ramey<sup>2</sup>, Joseph F. Georges<sup>1,3</sup>, Michael A. Mooney<sup>2</sup>, Nikolay L. Martirosyan<sup>2,4</sup>, Mark C. Preul<sup>1</sup>, Peter Nakaji<sup>2</sup>

<sup>1</sup>Neurosurgery Research Laboratory and <sup>2</sup>Division of Neurological Surgery, Barrow Neurological Institute, St. Joseph's Hospital and Medical Center, Phoenix, <sup>3</sup>School of Life Sciences, Arizona State University, Tempe, <sup>4</sup>Division of Neurosurgery, Department of Surgery, The University of Arizona, Tucson, AZ, Arizona, USA

E-mail: Aqib H. Zehri - [Neuropub@dignityhealth.org](mailto:Neuropub@dignityhealth.org); Wyatt Ramey - [Neuropub@dignityhealth.org](mailto:Neuropub@dignityhealth.org); Joseph Georges - [Neuropub@dignityhealth.org](mailto:Neuropub@dignityhealth.org); Michael Mooney - [Neuropub@dignityhealth.org](mailto:Neuropub@dignityhealth.org); Nikolay Martirosyan - [Neuropub@dignityhealth.org](mailto:Neuropub@dignityhealth.org); Mark Preul - [Neuropub@dignityhealth.org](mailto:Neuropub@dignityhealth.org);

\*Peter Nakaji - [Neuropub@dignityhealth.org](mailto:Neuropub@dignityhealth.org)

\*Corresponding author

Received: 20 November 13    Accepted: 13 February 2014    Published: 28 April 14

**This article may be cited as:**

Zehri AH, Ramey W, Georges JF, Mooney MA, Martirosyan NL, Preul MC, et al. Neurosurgical confocal endomicroscopy: A review of contrast agents, confocal systems, and future imaging modalities. *Surg Neurol Int* 2014;5:60.

Available FREE in open access from: <http://www.surgicalneurologyint.com/text.asp?2014/5/1/60/131638>

Copyright: © 2014 Zehri HA. This is an open-access article distributed under the terms of the Creative Commons Attribution License, which permits unrestricted use, distribution, and reproduction in any medium, provided the original author and source are credited.

### Abstract

**Background:** The clinical application of fluorescent contrast agents (fluorescein, indocyanine green, and aminolevulinic acid) with intraoperative microscopy has led to advances in intraoperative brain tumor imaging. Their properties, mechanism of action, history of use, and safety are analyzed in this report along with a review of current laser scanning confocal endomicroscopy systems. Additional imaging modalities with potential neurosurgical utility are also analyzed.

**Methods:** A comprehensive literature search was performed utilizing PubMed and key words: *In vivo* confocal microscopy, confocal endomicroscopy, fluorescence imaging, *in vivo* diagnostics/neoplasm, *in vivo* molecular imaging, and optical imaging. Articles were reviewed that discussed clinically available fluorophores in neurosurgery, confocal endomicroscopy instrumentation, confocal microscopy systems, and intraoperative cancer diagnostics.

**Results:** Current clinically available fluorescent contrast agents have specific properties that provide microscopic delineation of tumors when imaged with laser scanning confocal endomicroscopes. Other imaging modalities such as coherent anti-Stokes Raman scattering (CARS) microscopy, confocal reflectance microscopy, fluorescent lifetime imaging (FLIM), two-photon microscopy, and second harmonic generation may also have potential in neurosurgical applications.

**Conclusion:** In addition to guiding tumor resection, intraoperative fluorescence and microscopy have the potential to facilitate tumor identification and complement frozen section analysis during surgery by providing real-time histological assessment. Further research, including clinical trials, is necessary to test the efficacy of fluorescent contrast agents and optical imaging instrumentation in order to establish their role in neurosurgery.

**Key Words:** Brain neoplasm, confocal endomicroscopy, fluorescent dyes, intraoperative imaging, neuronavigation, optical imaging

Access this article  
online

Website:

[www.surgicalneurologyint.com](http://www.surgicalneurologyint.com)

DOI:

10.4103/2152-7806.131638

Quick Response Code:



## INTRODUCTION

Glioblastoma (GBM) is the most common primary malignant brain tumor with approximately 16,000 Americans diagnosed each year.<sup>[101]</sup> Following surgical resection of this tumor, the incidence of recurrence at the primary tumor site is greater than 80%, and the median patient survival is only 12.2-18.2 months.<sup>[58,117]</sup> GBM extent of resection is directly correlated with patient survival in some studies, with the maximum survival benefit achieved at greater than 98% tumor volume reduction.<sup>[56,85]</sup> Aggressive treatment with maximal resection plus adjuvant radiation and chemotherapy can increase patient survival by a range of 3-4 to 7-12 months.<sup>[118]</sup> While debate exists about the exact relationship between degree of resection and outcome, achieving maximal resection with minimal deficits remains a key neuro-oncological goal.

Such maximal resection is difficult to achieve due to the infiltrative nature of GBM and the need to preserve eloquent brain regions. Neurosurgeons use a variety of adjuncts such as intraoperative magnetic resonance imaging (MRI), neuronavigation, ultrasonography, and macroscopic fluorescence to help guide surgical resection, but none of these technologies provide detail at a cellular level.<sup>[98,107]</sup> A means for examining neoplastic tissue at a cellular level could improve differentiation between tumor and normal brain and facilitate tumor cytoreduction. Successfully making this distinction could contribute to a higher deficit-free resection rate. Arguably, actual visualization of neoplastic cells could be preferable to resecting the tumor to the margins defined by gadolinium-enhancement on MRI, which are known to not reflect the true extent of tumor.

Advancing optical technologies, such as a laser scanning confocal endomicroscopy (LSCE), provide real-time histopathological information of GBM *in vivo*. This technology has been used to distinguish diseased and normal tissue in other systems, including the gastrointestinal (GI) tract,<sup>[19,23,34,37]</sup> the cervix,<sup>[105]</sup> and the bladder.<sup>[120]</sup> LSCE allows microscopic tissue analysis with cellular and subcellular detail *in vivo*,<sup>[32,51]</sup> and contrast of morphological details can be enhanced with the application of exogenous fluorescent dyes.<sup>[33]</sup> This technology has recently been studied in the neurosurgical setting in an effort to improve tumor resection by providing immediate histological assessment of the brain-to-neoplasm interface.<sup>[28,64,88,89]</sup>

In this review, we assess the properties and utility of each of the three fluorophores currently available for neurosurgical clinical use, as well as the specifications of the two currently available LSCE systems. Additionally, future optical technologies currently under investigation are discussed in relation to neurosurgical applications.

## CLINICALLY AVAILABLE EXOGENOUS AGENTS

Exogenous dyes effective for neurosurgical applications require neurolocalization and selective contrast of neurohistopathological structures. Theoretically, effective tumor targeting occurs through enhanced permeability and retention, where vascular proliferation and anatomical abnormalities (such as limited lymphatic drainage and venous return) allow exogenous agents to concentrate at the tumor site.<sup>[14,36,46,61,67,93,103]</sup> Thus, the breakdown of the blood-brain barrier in glioma allows exogenous dyes to concentrate in neoplastic regions and contrast abnormal tissue.<sup>[79]</sup>

The Stokes shift describes the relationship between single photon excitation and emission of fluorophores, which is absorption of short-wavelength (higher energy) photons and emission of longer wavelength (lower energy) photons.<sup>[76]</sup> Each exogenous dye has specific absorption and emission spectra, which can be filtered to visualize the fluorescent contrast agent in susceptible tissues.<sup>[108]</sup>

Properties of effective exogenous fluorescent agents include minimal phototoxicity, scattering, and signal attenuation. Phototoxicity occurs with fluorophore excitation and resultant production of reactive oxygen species (ROS),<sup>[4,20,29,43,63,115,121]</sup> which can damage cellular structures and reduce the signal of the fluorophore, leading to photobleaching.<sup>[6,94,95]</sup> Ideal fluorophores have a high quantum yield (i.e. a high ratio of emitted fluorophores to absorbed fluorophores).<sup>[108]</sup>

Scattering, signal attenuation, and native autofluorescence all limit the depth at which a fluorophore can be visualized within tissue.<sup>[31,59]</sup> Scattering and native autofluorescence decrease as wavelength increases, with the infrared emission spectra (700-900 nm) being ideal for imaging deeper cellular structures.<sup>[30,108]</sup>

## FLUORESCEIN SODIUM

### Optical and chemical properties

Fluorescein sodium is a small organic molecular salt that has an excitation maximum of 494 nm and an emission maximum of 521 nm.<sup>[79]</sup> It readily crosses capillaries, provides fluorescent contrast in the extracellular matrix,<sup>[71]</sup> and has a urine clearance of 24-36 h after intravenous injection.<sup>[79]</sup> The amount of fluorescein delivered to a tumor site is increased by the breakdown of the normal blood-brain barrier, which becomes useful in neurosurgical applications.<sup>[5]</sup>

### Neurosurgical applications

Fluorescein sodium has been approved by the United States Food and Drug Administration (FDA) for ophthalmoscopic examinations of the retina since the 1960s.<sup>[5,92]</sup> In the field of neurosurgery, fluorescein

has been used in cerebral angiography to detect arteriovenous malformations,<sup>[26]</sup> superficial temporal artery-middle cerebral artery anastomoses,<sup>[60]</sup> and to aid in treating cerebral aneurysms.<sup>[122]</sup>

Fluorescein was first reported to contrast brain tumors in a 1948 study showing tumor visualization in 95.7% of patients.<sup>[69]</sup> This demonstrated the ability of fluorescein to localize at the site of the tumor, mainly due to breakdown of the normal blood-brain barrier.<sup>[52]</sup> Thus, fluorescein is not a tumor-specific agent, but it is excellent for visualizing regions of compromised neurovasculature. The presumption in its use for neuro-oncology is that these areas correspond to the enhancing regions, which also correspond to bulk tumor. It is believed that fluorescein does not differentially leak into and stain tumor cells that have infiltrated beyond the gross enhancing margin.<sup>[92]</sup> However, resection of these cells within otherwise normal surrounding brain may also raise the risk of neurological deficit.

Several decades later, fluorescein was utilized to macroscopically demarcate brain tumors during resection under white light without surgical microscopes.<sup>[10,53,70,74,92]</sup> One study reported that gross total resection (GTR) of GBM was achieved in 84.4% of patients who received fluorescein compared with only 30.1% of patients who did not.<sup>[92]</sup> These results were reproduced in a prospective study;<sup>[53]</sup> however, it should be noted that both studies failed to show a significant survival benefit despite higher rates of GTR in patients who received fluorescein. In a separate study of low-grade gliomas, use of fluorescein was shown to significantly increase the achievement of GTR, as well as to increase 6-month progression-free survival.<sup>[10]</sup> This technique has been considered safe to use, easy to perform, and requires no extra surgical equipment for tumor resection.<sup>[79]</sup> However, the extent of resection and visualization of the tumor border is dependent on the surgeon's judgment of fluorescence, which may be limited in tumor areas with intact vasculature.

In 1998, a modified surgical microscope was developed equipped with dichroic mirrors specific for fluorescein-guided resection of malignant gliomas.<sup>[55]</sup> This system allowed more accurate demarcation of tumor boundaries and reduced the amount of fluorescein given when compared with studies that visualized tumor macroscopically.<sup>[5]</sup> The study reported 100% gross GTR resection in all patients, except those patients with tumors in eloquent areas, such as the basal ganglia and brain stem, which limited the resection.

LSCE was first used to image GBM in animal models in 2010.<sup>[88]</sup> Using fluorescein delivered intravenously, researchers were able to distinguish between tumor and nontumor regions using a handheld confocal microscope. This technology identified infiltrating tumor margins at a cellular level *in vivo* for the first time. Another study conducted with fluorescein-guided LSCE demonstrated

the ability of histological *in vivo* imaging of normal and neoplastic tissue in rat allograft models *in vivo* and human tissue *ex vivo*.<sup>[25]</sup> *In vivo* fluorescein staining depicted tissue morphology and cellular structures as well as capillaries in normal tissue, while showing rapid tumor growth and massive extravasation in the region of the tumor. Fluorescein application *ex vivo* allowed the diagnosis of various brain tumor subtypes, not only GBM, using LSCE. However, there was limited depth perception, and it was noted that near-infrared probes may solve this issue.<sup>[108]</sup>

Also in 2010, fluorescein-guided LSCE technology was utilized in a human trial, and it provided assessment of tumor grade, tumor histology, and tumor margins for a variety of tumor subtypes.<sup>[86]</sup> Following this proof-of-principle study, a larger study imaging various brain tumors including meningiomas, schwannomas, gliomas of various grades, and a hemangioblastoma was performed.<sup>[24]</sup> LSCE with fluorescein was able to correctly diagnose and correspond with traditional histopathological findings with an accuracy of 92.9% when the pathologist was given a list of clinically relevant diagnoses to choose from. Though interpretation was somewhat biased toward

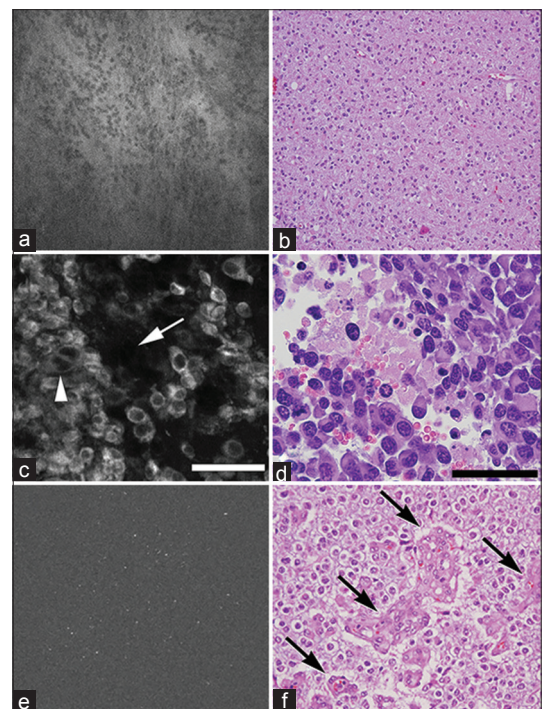


**Figure 1:** Images obtained with intraoperative endomicroscopes of various clinically available fluorescent contrast agents. (a and b) Fluorescein-induced fluorescence of oligodendroglioma (Grade II), and corresponding H and E stain. (c and d) ICG-induced fluorescence of glioblastoma cells in a mouse model, and corresponding H and E stain. (e and f) 5-ALA induced fluorescence in low-grade glioma, and corresponding H and E stain. Figures a and b from Eschbacher et al.,<sup>[24]</sup> used with permission from Journal of Neurosurgery. Figure c used with permission from Barrow Neurological Institute. Figure d from Martirosyan et al.,<sup>[64]</sup> used with permission from Journal of Neurosurgery. Figures e and f from Sanai et al.,<sup>[87]</sup> used with permission from Journal of Neurosurgery



a list of potential pathologies, this technology was able to give a good direction toward the final diagnosis and intraoperatively discern regions of tumor infiltration in both low- and high-grade gliomas [Figure 1a and b]. In this study, LSCE images were collected in grayscale, however, they can be pseudocolored for ease of interpretation by a clinician. The results from these two studies demonstrate the feasibility of this technology as a diagnostic and therapeutic tool, as it can help identify many of the pathognomonic cytoarchitectural features of various brain tumors and aid in the intraoperative diagnosis and resection of various central nervous system (CNS) tumors. Fluorescein in this case can both guide the operator grossly to areas to be viewed with LSCE and provide the contrast to allow cellular visualization. The next phase in validation of this technique is to provide optical “biopsies”, which can then be compared in blinded fashion against frozen section, to evaluate its overall diagnostic accuracy.

### Safety

Fluorescein is FDA approved and is widely used in the field of ophthalmology as well as in GI studies.<sup>[55,116]</sup> Most fluorescein clinical studies in neurosurgery report no serious adverse effects with use of the fluorophore,<sup>[11,53,70,74,92]</sup> however, in an international study using fluorescein, 1.4% of patients developed minor complications such as nausea and vomiting.<sup>[5]</sup> No patients suffered severe adverse events in this study. Deleterious effects can occur with rapid high dose administration (20 mg/kg) of fluorescein,<sup>[90]</sup> but these high doses can be avoided when fluorescein is imaged using a surgical microscope that requires less dosage compared with macroscopic viewing.<sup>[55,69]</sup>

## INDOCYANINE GREEN

### Optical and chemical properties

Indocyanine green (ICG) is a near-infrared fluorescent agent with maximal excitation at 778 nm and emission spectra range of 700-850 nm in serum.<sup>[38,59,72,73]</sup> It is fairly water-soluble, which allows it to be given intravenously and cleared through renal and bile excretion.<sup>[30,80]</sup> ICG concentration within a tumor site is enhanced by breakdown of the normal blood-brain barrier. ICG has a greater tissue penetrance than visible-wavelength fluorophores, such as 5-ALA and fluorescein. ICG is an anionic, amphiphilic, tricarboyanine probe, which allows it to have a high affinity for proteins, such as albumin, and allows visualization of solid tumors, but may also cause higher levels of nonspecific binding.<sup>[5]</sup> Similar to fluorescein, ICG provides nonspecific contrast in areas of permeable neurovasculature.<sup>[78,108]</sup>

### Effectiveness in neurosurgical applications

ICG has been given intravenously for blood vessel angiography,<sup>[16,1,65,81,106]</sup> identifying extrahepatic bile

ducts<sup>[66]</sup> and detecting liver metastases.<sup>[2]</sup> It can also be given subcutaneously for sentinel lymph node mapping for breast, anal, and GI cancer<sup>[42,49,73,80,104]</sup> as well as assessing lymphatic drainage for lymphedema.<sup>[90]</sup>

The first application of ICG for macroscopic demarcation of glioma tumor margins was investigated in 1993.<sup>[40]</sup> The results demonstrated that ICG was able to contrast the fluorescent tumor tissue within 1 mm of the histological tumor margins in an animal model. However, this technique is not effective in distinguishing between malignant cells and other areas of the brain that may incidentally uptake the injected dye. Cellular visualization using ICG contrast may overcome these limitations.<sup>[39]</sup>

With the development of an infrared LSCE, ICG was first investigated *in vivo* to diagnose liver steatosis and fibrosis.<sup>[32]</sup> Recently, ICG has proven useful in neurosurgical applications. In animal glioma models, ICG imaging with a near-infrared wavelength confocal endomicroscope has been effective at detecting tumor, transitional zones, and normal brain [Figure 1c and d].<sup>[64]</sup> LSCE technology can confirm, at the cellular level, regions fluorescently labeled with ICG are truly representative of the tumor. In contrast, macroscopic detection is more subjective to the surgeon. Intravenously administered ICG is immediately localized to a tumor site, and the fluorescent signal remains in the tumor up to 1 h after injection, with constant imaging, demonstrating limited photobleaching and clearance. The delivery of the dye to the site of the tumor relies on binding to serum proteins<sup>[3]</sup> and the damaged vasculature primarily located at the site of the tumor. However, with time the dye will diffuse into surrounding tissue.<sup>[64]</sup> These properties allow real-time, *in vivo* assessment that differentiates glioma tissue and normal brain. In contrast to visible wavelength fluorophores, ICG provides visualization of deeper tissue structures due to its infrared excitation and emission spectra. However, depth of imaging still remains limited to a few hundred microns deep to the imaging surface.

### Safety

Intravenous injection of ICG is approved by the FDA for several clinical applications, including cerebrovascular surgery, and has been shown to have a low negative-reaction profile.<sup>[16,80,81]</sup> Toxicities and risk for anaphylactic shock have been reported at high doses, however, and off-label use must be undertaken with caution.<sup>[2,75]</sup> Despite these considerations, ICG is considered to have fewer risks than other FDA approved intravenous fluorophores.<sup>[64]</sup>

## AMINOLEVULINIC ACID (5-ALA)

### Optical and chemical properties

Produced in the mitochondria, 5-ALA is a natural precursor for the production of protoporphyrin IX (PpIX)

in the heme synthesis pathway found in all cells.<sup>[54,79]</sup> PpIX is a fluorescent molecule that binds membrane lipids and has an excitation range of 375-440 nm and emission range of 640-710 nm *in vivo*.<sup>[12,54,99]</sup> Overloading this pathway with exogenous 5-ALA causes the collection of PpIX to fluorescently detectable levels in cells.<sup>[50,77]</sup> As the production of PpIX occurs *in situ* in mitochondria, fluorescence is limited to cells. This decreases fluorescent signal in blood or edematous regions of the operative field.<sup>[98]</sup> Furthermore, neoplastic cells demonstrate preferential uptake of exogenous 5-ALA and increased collection of PpIX, making the fluorescent signal more robust in these abnormal tissues and making intraoperative visualization feasible, especially in intracranial tumors of higher grades.<sup>[12]</sup>

Photobleaching occurs with PpIX fluorescence level dropping to 36% after 25 min under violet light or 87 min under white light.<sup>[112]</sup> It can be limited by allowing excitation and white light to penetrate as small an area as possible in the surgical field.<sup>[12]</sup> Phototoxicity is limited with 5-ALA, since fluorescent microscopes do not produce sufficient energy for significant ROS production.<sup>[100]</sup>

### Neurosurgical application

Due to its favorable optical and chemical properties, clinical applications of 5-ALA have been extensively studied in an array of medical specialties and a variety of tissues. Currently, the FDA has approved 5-ALA and its derivatives for research diagnostic applications in endoscopic, photodynamic detection of bladder cancer and residual glioma, as well as the treatment of basal cell carcinoma and actinic keratosis.<sup>[54]</sup>

The first study of 5-ALA-induced fluorescence of human gliomas was reported in 1998.<sup>[100]</sup> After oral administration of 5-ALA, PpIX fluorescence was exclusively observed in tumor regions using a surgical microscope modified for fluorescence. Histological analysis demonstrated 85% sensitivity, 100% specificity, and 90% accuracy for predicting the presence of malignant tissue from 5-ALA-induced macrofluorescence in this study. Photobleaching and spontaneous deterioration occurred in this study with excessive exposure to light. Necrotic and edematous regions had little fluorescence. Overall, the study revealed a high degree of congruity between macroscopic visualization of PpIX fluorescence and the presence of neoplastic tissue. However, the investigators did not determine the outcome of 5-ALA-guided tumor resection.

A follow-up study using similar operative methods was undertaken to determine the efficacy of fluorescence-guided resection with 5-ALA in 52 patients with GBM.<sup>[98]</sup> This study showed that GTR was achieved in 63% of patients. Postoperative residual tumor was also assessed with contrast-enhanced MRI, which proved to

be less sensitive in showing residual tumor compared with fluorescent enhancement of glioma *in vivo*.<sup>[5]</sup> Finally, the level of residual solid tissue fluorescence was shown to correlate with patient survival: Patients with minimal to no fluorescence had higher survival rates than those with high levels of fluorescence postoperatively.

The results from this study led to a randomized controlled trial that further determined the efficacy and safety of 5-ALA-induced macrofluorescence-guided GBM resection.<sup>[98,99]</sup> The phase III clinical trial with 322 patients demonstrated greater tumor resection using this technique compared with patients who underwent conventional microsurgery under white light (65% vs. 36% GTR). Overall progression-free survival time also increased by 1.5 months in groups administered 5-ALA, which included an increase of 6 months in the subgroup of patients over 55.<sup>[70]</sup> Though survival time increased, quality of life was not measured and may be an important factor in deciding tumor resection strategy when using this technology.

While 5-ALA-induced fluorescence is successful for both diagnosis and resection of high-grade gliomas, there are many studies reporting that macroscopically detectable fluorescence does not occur in low-grade gliomas.<sup>[27,45]</sup> Therefore, an investigation was conducted utilizing a hand held intraoperative confocal microscope to visualize low-grade gliomas after standard administration of 5-ALA.<sup>[87]</sup> This technology allowed visualization of 5-ALA-induced fluorescence of low-grade glioma tumor and tumor margins *in vivo* that corresponded with standard histopathology [Figure 1e and f]. Overall, both pre- and postoperative MRI in 10 patients indicated a median of 95% extent of tumor resection using this imaging modality. This technology may permit intraoperative fluorescence contrast of low-grade gliomas if necessitated in the treatment plan of a patient. Some controversy still exists as to the biology of 5-ALA metabolism in low-grade gliomas and the need for complete resection by MRI. However, as the distinction between low-grade glioma and surrounding brain can be especially challenging, this remains an important area for future work.

### Safety

Though 5-ALA administration is considered safe,<sup>[99]</sup> minor systemic side effects have been reported, including nausea, vomiting, and hypotension as well as increased sensitivity to sunlight up to 48 h after administration.<sup>[12]</sup> As with other fluorophores, these side effects are limited with lower dosing.

## INTRAOPERATIVE ENDOMICROSCOPY SYSTEMS

Commercially introduced in the 1980s, confocal microscopy has been extensively used for molecular

imaging of thick tissues in the biomedical sciences. Miniaturization of this technology into an endoscope (LSCE) was fueled by a need to diagnose *in vivo* premalignant lesions in epithelial cancers.<sup>[9]</sup> LSCE has been extensively tested for visualizing Barrett's esophagus, urothelial bladder neoplasia, and cervical intraepithelial neoplasia.<sup>[23,105,120]</sup>

LSCE provides noninvasive histological images *in vivo* through optical sectioning.<sup>[57,109]</sup> Optical sectioning allows the microscope to selectively image a certain focal depth by mechanically filtering most out-of-focus photons above and below the focal plane with a pinhole.<sup>[48]</sup> This enables imaging of thick tissue with greater contrast compared with conventional wide-field microscopy, which generates out-of-focus background light and scatter.<sup>[13]</sup> Furthermore, endomicroscopy allows for three dimensional image reconstruction and greater imaging parameters.<sup>[13]</sup> Most importantly, this technology permits real-time histopathological analysis with increased diagnostic yield without the traditional histopathological process of excision, fixation, and staining.

While neurosurgeons are equipped with macroscopic fluorescence-guided surgery, the distinction of healthy and tumor cells remains a challenge for immediate tumor distinction during tumor resection. Therefore, the application of this technology may provide novel cellular details of CNS tumor architecture. Confocal endomicroscopy using fluorescent dyes has successfully been researched in the imaging and resection of brain tumors *in vivo* in animal models and to some extent in human subjects.<sup>[86-88]</sup> These results demonstrate *in vivo* visualization of brain tumors using fluorophores. Specifically, 5-ALA and LSCE systems can facilitate intraoperative diagnosis and real-time, fluorescence-guided resections of brain tumors. Further clinical trials are needed for nonspecific fluorescent agents, such as ICG and fluorescein that accumulate in the extracellular compartment. There are two clinically available confocal endomicroscopy systems, which are assessed in this review for their possible application for neurosurgical purposes: Optiscan/Pentax ISC-1000 and Mauna Kea Cellvizio.

### Optiscan

The Optiscan is a conventional endoscope with a miniaturized confocal microscope at the tip designed mainly to image the lower GI tract, but has also been used for imaging of the stomach, duodenum, distal esophagus, and the cervix.<sup>[48]</sup> This system provides excellent image clarity but requires image stabilization.<sup>[22]</sup> The miniature confocal microscope scanner is within a rigid probe that is connected to an optical unit and PC unit via a flexible umbilicus [Figure 2a]. The probe uses a distal scanner with a single optical fiber, which contains both excitation and detection capability.<sup>[48]</sup> A miniaturized objective

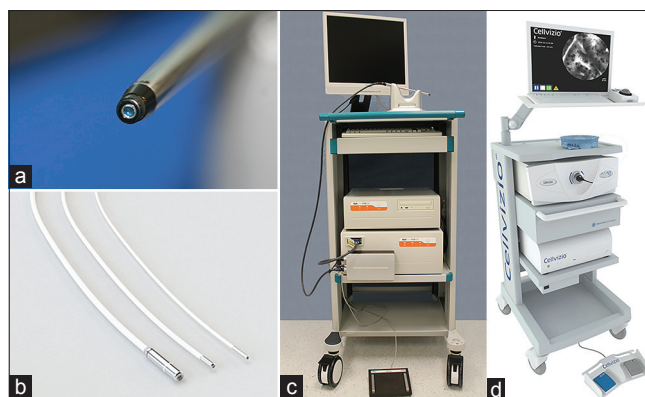


**Figure 2: Clinically available laser scanning confocal endomicroscopy systems. (a)** The Optiscan system has a single probe with a distal tip diameter of 5.0 mm, length of 150 mm and 300 mm, and a field of view of  $475 \times 475 \mu\text{m}$ . Working distance can be adjusted from the surface to  $250 \mu\text{m}$ . **(b)** Cellvizio has a range of miniprobes available for imaging various organs, including brain, each with various imaging depths, distal tip diameter, lateral and axial resolution, and field of view. **(c)** The main unit, Pentax ISC-1000, provides the excitation light source, a foot pedal to adjust the depth of confocal imaging penetration, and an imaging screen. **(d)** The Cellvizio laser scanning unit provides the laser source and a surgical-grade screen. The unit comes with the Cellvizio Software that can record, export, and modify images. A foot pedal allows the user to start and stop the acquisition and to save images to a hard drive. Figures a and c used with permission from Barrow Neurological Institute. Figures b and d used with permission from Mauna Kea Technologies

lens comes into direct contact with tissue, creating a  $475 \times 475\text{-}\mu\text{m}$  field of view. The operator is able to control the focus depth through a foot pedal at  $4\text{-}\mu\text{m}$  steps anywhere from 0 to  $250 \mu\text{m}$  beyond the window surface<sup>[48]</sup> [Figure 2c]. Similar to the Cellvizio LSCE, both the excitation light and the emitted fluorescence are transduced and collected at the same point, which in this case is the single optical fiber. 488-nm excitation is emitted from the solid-state laser with a maximum power of 1 mW, while light at wavelengths outside the red-violet spectrum is filtered during detection, limiting perceived fluorescence to wavelengths of 505-705 nm.<sup>[24,87]</sup> The Optiscan collects images at a rate of up to 0.7 frames per second. A customized rigid Optiscan probe was used in the fluorescein LSCE study by Eschbacher *et al.*<sup>[24]</sup>

### Cellvizio

The Cellvizio LSCE is a probe-based endomicroscopy system that has been used for *in vivo* imaging of the upper and lower GI tract, as well as the human bladder.<sup>[22,84,96]</sup> Because of its compact size and maneuverability, this system is well-suited for microsurgical and experimental imaging techniques, such as examination of microvasculature, detection of dysplastic cells, and observation of neuroblast migration.<sup>[17,44,57]</sup> The system also incorporates a range of miniprobes that can be inserted into an endoscope or used independently.<sup>[48]</sup> [Figure 2b]. There are various miniprobes that differ in their field of view, fixed working distance, and lateral and axial resolution.



Each miniprobe has specific applications based on these technical parameters, one of which is designated for imaging the surface of the brain. The system as a whole can collect full frame images at 12 frames per second.<sup>[48]</sup> The Cellvizio LSCE is composed of three main components: (i) a laser optoelectric unit, (ii) an array of optical fiber mini-probes linking the proximal scanning device and the micro-objective, and (iii) software that controls the system and manages the image data<sup>[57]</sup> [Figure 2d]. A 488- or 660-nm laser source provides the excitation light. Real-time imaging is accomplished with a 4-kHz oscillating mirror for horizontal scanning and a galvanometric mirror for frame scanning, resulting in a frame rate of 12 Hz.<sup>[57]</sup> The same fiber bundle that is used for illumination of the specimen collects fluorescence that is then diverted to the photodetector. The resultant raw image is first processed using an algorithm designed to eliminate inherent artifact resulting from the fiber optic bundles. Therefore, the system is first calibrated by measuring intrinsic autofluorescence of each fiber by imaging a nonfluorescent sample, in addition to the transmission and collection rate of each fiber.<sup>[57]</sup> Distortions generated by the system can then be accounted for, thereby providing images capable of quantitative measurements.

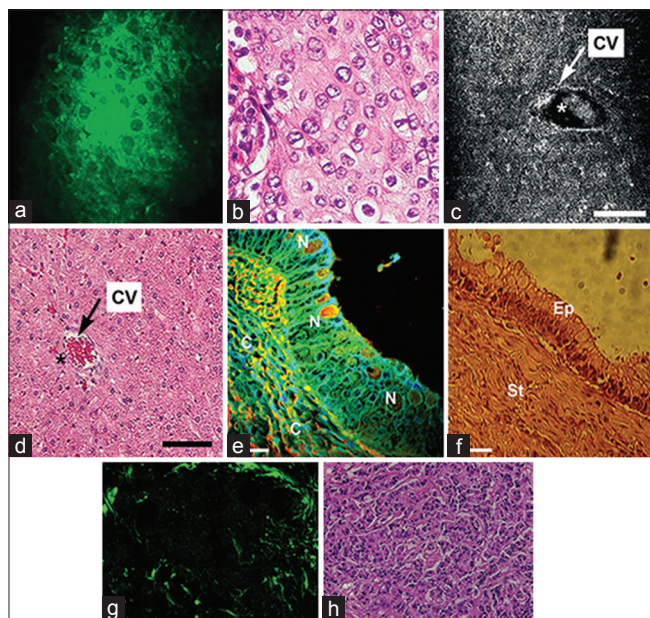


**Figure 3: Emerging optical technology with possible neurosurgical applications. (a and b) Coherent anti-Stokes Raman scattering (CARS) microscopy of human lung squamous cell carcinoma ex vivo and corresponding H and E stain. (c and d) Near-infrared confocal reflectance microscopy of rat liver ex vivo, and corresponding H and E stain. (e and f) Fluorescence lifetime microscopy of mucinous ovarian tumor ex vivo, and corresponding H and E stain. (g and h) Two-photon microscopy of human breast cancer ex vivo, and corresponding H and E stain. Figures a and b from Gao et al.<sup>[124]</sup> (open access). Figures c and d from Campo-Ruiz et al.,<sup>[7]</sup> reprinted by permission from Macmillan Publishers Ltd: Modern Pathology, copyright 2005. Figures e and f from Adur et al.<sup>[125]</sup> (open access). Figures g and h from Wu et al.<sup>[126]</sup> (open access)**

## FUTURE DEVELOPMENTS

### Coherent anti-Stokes Raman scattering microscopy

Similar to MRI, coherent anti-Stokes Raman scattering (CARS) microscopy is a microscopy technique that produces an image based on intrinsic vibratory properties of the specimen. Using an oscillating laser system that produces molecular vibration in the specimen and a modified beam-scanning commercial microscope that detects the resonance of “anti-Stokes” oscillating molecules, detailed images of normal brain structures [Figure 3a and b], as well as margins of intracranial gliomas, can be generated.<sup>[2]</sup> These images have been shown to be both sensitive and specific for cancerous tissue at the cellular level. CARS depict the microenvironment and cellular morphology that can potentially provide the investigator with a means of diagnosis without the need for biopsy and hematoxylin and eosin staining. Therefore, in addition to the benefit of discerning normal versus pathologic CNS tissue *in vivo* for tumor resection, there is a diagnostic capability to CARS as well.<sup>[91]</sup> However, further development of CARS for the *in vivo* neurosurgical setting will require its miniaturization for practical uses in the operating room.

### Confocal reflectance microscopy

Using light scattering technology, confocal reflectance microscopy (CRM) is an imaging technique that noninvasively images a thin plane of tissue with high resolution.<sup>[7,111]</sup> CRM generates contrast by utilizing the intrinsic differences in refractivity of targeted tissue. Images are generated with relatively lower refractive structures contributing fewer signals in the resultant image.<sup>[7]</sup> Since CRM does not rely on a Stoke’s shift, it introduces a fraction of energy into tissue samples compared with fluorescence imaging techniques.<sup>[7]</sup> Overall, this technique allows real-time analysis of tissue cellularity and cytoarchitecture with minimal production of ROS.<sup>[7,111]</sup> Limitations of CRM technology include limited depth (200-300  $\mu\text{m}$ ) and sharpness to evaluate intracellular structures. Imaging depth can be increased with increasing wavelengths, but can compromise resolution and contrast.<sup>[111]</sup>

CRM has been investigated to image cellular and subcellular tissue architecture, diagnose dermatological conditions noninvasively, identify cancerous tissue and margins intraoperatively, and assess cellular and subcellular detail of diseased and normal hepatic tissue<sup>[7,8,11,15,21,35,41,82,111,119]</sup> [Figure 3c and d]. CRM has recently been used to determine the cellularity *ex vivo* of brain tumor specimens.<sup>[123]</sup> Successful application of this imaging technique in the field of glioma surgery could provide faster throughput sampling from the surgical field and increase diagnostic yield.

### Fluorescence lifetime imaging

Fluorescence lifetime imaging (FLIM) generates contrast by measuring the length of time a fluorophore remains in its excited state. By adding the extra dimension of time, FLIM provides a more specific means of identifying tumor cells based on the inherent amount of time endogenous fluorophores continue to emit photons. An alternative to measuring fluorescence intensity alone, FLIM capitalizes on the finite high-energy state by essentially averaging its lifetime in the tissues following excitation from the ground state, demonstrating relatively longer lifetime values in tumor cells<sup>[62]</sup> [Figure 3e and f]. This is particularly useful in autofluorescence since many endogenous molecules possess overlapping spectra of fluorescence, thereby increasing the parameters needed for optimal contrast. Recently, FLIM has been used for identifying oral precancerous lesions, skin lesions due to UVB radiation, and in determining the function of retinal pigment cells.<sup>[47,68,97]</sup> The first use of FLIM for brain tumor image-guided surgery in humans showed that GBM had a significantly more irregular excitation lifetime distribution as compared to normal cortex.<sup>[102]</sup> While these results indicate the feasibility of such a time-dependent imaging modality in brain tumor resection, there exist several limitations for potential larger-scale *in vivo* human surgical trials, such as the lengthy time needed to acquire images, the complicated equipment that must be maneuvered and operated, and the cost of the procedure.<sup>[47]</sup>

### Two-photon and second harmonic generation

While the depth of imaging limits confocal and other types of linear fluorescence microscopy, two-photon microscopy has the distinct advantage of visualizing deep cellular structures [Figure 3g and h]. With concentrated photons pulsed from a femtosecond laser, two photons, each containing approximately half of the energy required to linearly excite the fluorophore, simultaneously interact with the same molecule.<sup>[114]</sup> Intensity of these pulsed photons decreases circumferentially around the area of focus, resulting in a small volume of fluorescence emitting directly from the focal point. This allows spatial restriction of fluorescence to the focal point with reduced scattering. Additionally, two-photon microscopy uses infrared and far-red excitation wavelengths, which provide greater tissue penetration compared with the more superficial use of visible wavelength light.<sup>[114]</sup>

Another nonlinear imaging modality is second harmonic generation (SHG). This modality generates contrast based on the degree of photon scattering when incident photons interact with heterogeneous tissue. Although two photons with half the expected energy also interact at the focal point in SHG, they only do so after they are scattered by the same molecule rather than absorbed. This “emitting” photon with essentially twice the energy is then detected creating an image with potential for

*in vivo* use during surgery. However, further development of such technologies is needed, including improvement of image processing time and spatial recognition issues.<sup>[83]</sup>

### CONCLUSION

Currently, the frozen section provides intraoperative histopathological analysis of brain tumors. Though useful, this process is time consuming and requires the cutting, freezing, and staining of several biopsies. Frozen section sample preparation frequently damages tissue, alters cellular architecture, and introduces tissue artifacts, all of which hinder a proper diagnosis.<sup>[110,113]</sup> Application of exogenous fluorophores approved for neurosurgery and miniaturization of confocal microscopy may overcome the limitations of traditional intraoperative histopathology. Future operating rooms may see the routine use of fluorescence confocal endomicroscopes and clinically approved contrast agents, as well as the development of training programs to educate pathologists and surgeons to effectively apply this technology. The translation of this technology for neurosurgical use could improve patient care by providing the neurosurgeon with real-time histopathological information from more regions of interest than are possible with frozen section analysis.

Fluorophores approved for clinical neurosurgery include 5-ALA, fluorescein, and ICG. 5-ALA provides tumor-specific labeling for macroscopic detection of brain tumors. 5-ALA has been clinically used with fluorescence surgical microscopes to enhance the extent of resection of low-grade gliomas, which have limited uptake of 5-ALA. Confocal endomicroscopy with 5-ALA may provide visualization of tumors at the cellular level, which will allow real-time differentiation between normal and malignant cells. Fluorescein and ICG, provide less tumor-specific staining, and have demonstrated the ability to macroscopically demarcate brain tumors due to the permeability of tumor vasculature. Both of these fluorophores have been studied with fluorescence endomicroscopy. Using this technology, fluorescein and ICG generate contrast and allow the *in vivo* histopathologic visualization of tissue cellularity and intercellular architecture. Compared with fluorescein, ICG provides greater depth of imaging due to its excitation-emission wavelengths in the infrared spectra, thereby minimizing scatter and autofluorescence.

Optiscan and Cellvizio each produce commercially available confocal endomicroscopy systems for clinical use. Both utilize different imaging software and technical specifications to accomplish the goal of providing *in vivo* cellular detail during surgical procedures. These systems have shown utility in studies related to epithelial-derived structures. However, more rigorous studies such as human clinical trials with clinically approved fluorophores are required to establish the efficacy of these systems in



the neurosurgical field. Novel imaging modalities are being studied in different organ systems. Investigation of future-imaging technologies in the field of neurosurgery is important for identifying new imaging tools available during neurosurgical procedures.

## REFERENCES

- Alford R, Simpson HM, Duberman J, Hill GC, Ogawa M, Regino C, et al. Toxicity of organic fluorophores used in molecular imaging: Literature review. *Mol Imaging* 2009;8:341-54.
- Aoki T, Yasuda D, Shimizu Y, Odaira M, Niiya T, Kusano T, et al. Image-guided liver mapping using fluorescence navigation system with indocyanine green for anatomical hepatic resection. *World J Surg* 2008;32:1763-7.
- Baker KJ. Binding of sulfobromophthalein (BSP) sodium and indocyanine green (ICG) by plasma alpha-1 lipoproteins. *Proc Soc Exp Biol Med* 1966;122:957-63.
- Bartosz G. Oxidative stress in plants. *Acta Physiol Plant* 1997;19:47-64.
- Behbahaninia M, Martirosyan NL, Georges J, Udovich JA, Kalani MY, Feuerstein BG, et al. Intraoperative fluorescent imaging of intracranial tumors: A review. *Clin Neurol Neurosurg* 2013;115:517-28.
- Bernas T, Zarebski M, Dobrucki JW, Cook PR. Minimizing photobleaching during confocal microscopy of fluorescent probes bound to chromatin: Role of anoxia and photon flux. *J Microsc* 2004;215:281-96.
- Campo-Ruiz V, Lauwers GY, Anderson RR, Delgado-Baeza E, González S. *In vivo* and *ex vivo* virtual biopsy of the liver with near-infrared, reflectance confocal microscopy. *Mod Pathol* 2005;18:290-300.
- Campo-Ruiz V, Ochoa ER, Lauwers GY, González S. Evaluation of hepatic histology by near-infrared confocal microscopy: A pilot study. *Hum Pathol* 2002;33:975-82.
- Carignan CS, Yagi Y. Optical endomicroscopy and the road to real-time, *in vivo* pathology: Present and future. *Diagn Pathol* 2012;7:98.
- Chen B, Wang H, Ge P, Zhao J, Li W, Gu H, et al. Gross total resection of glioma with the intraoperative fluorescence-guidance of fluorescein sodium. *Int J Med Sci* 2012;9:708-14.
- Clark AL, Gillenwater AM, Collier TG, Alizadeh-Naderi R, El-Naggar AK, Richards-Kortum RR. Confocal microscopy for real-time detection of oral cavity neoplasia. *Clin Cancer Res* 2003;9:4714-21.
- Colditz MJ, Leyen K, Jeffree RL. Aminolevulinic acid (ALA)-protoporphyrin IX fluorescence guided tumour resection. Part 2: Theoretical, biochemical and practical aspects. *J Clin Neurosci* 2012;19:1611-6.
- Conchello JA, Lichtman JW. Optical sectioning microscopy. *Nat Methods* 2005;2:920-31.
- Courtice F. The origin of lipoproteins in lymph. Springfield, Ill: Charles C. Thomas; 1968. p. 89-126.
- Curiel-Lewandrowski C, Williams CM, Swindells KJ, Tahan SR, Astner S, Frankenthaler RA, et al. Use of *in vivo* confocal microscopy in malignant melanoma: An aid in diagnosis and assessment of surgical and nonsurgical therapeutic approaches. *Arch Dermatol* 2004;140:1127-32.
- Dashti R, Laakso A, Niemela M, Porras M, Hernesniemi J. Microscope-integrated near-infrared indocyanine green videoangiography during surgery of intracranial aneurysms: The Helsinki experience. *Surg Neurol* 2009;71:543-50.
- Davenne M, Custody C, Charneau P, Lledo PM. *In vivo* imaging of migrating neurons in the mammalian forebrain. *Chem Senses* 2005;30 Suppl 1:i115-6.
- De Grand AM, Frangioni JV. An operational near-infrared fluorescence imaging system prototype for large animal surgery. *Technol Cancer Res Treat* 2003;2:553-62.
- Deinert K, Kiesslich R, Vieth M, Neurath MF, Neuhaus H. *In vivo* microvascular imaging of early squamous-cell cancer of the esophagus by confocal laser endomicroscopy. *Endoscopy* 2007;39:366-8.
- Dixit R, Cyr R. Cell damage and reactive oxygen species production induced by fluorescence microscopy: Effect on mitosis and guidelines for non-invasive fluorescence microscopy. *Plant J* 2003;36:280-90.
- Drezek RA, Richards-Kortum R, Brewer MA, Feld MS, Pitris C, Ferenczy A, et al. Optical imaging of the cervix. *Cancer* 2003;98 (9 Suppl):2015-27.
- Dunbar K, Canto M. Confocal endomicroscopy. *Curr Opin Gastroenterol* 2008;24:631-7.
- Dunbar KB, Okolo P, III, Montgomery E, Canto MI. Confocal laser endomicroscopy in Barrett's esophagus and endoscopically inapparent Barrett's neoplasia: A prospective, randomized, double-blind, controlled, crossover trial. *Gastrointest Endosc* 2009;70:645-54.
- Eschbacher J, Martirosyan NL, Nakaji P, Sanai N, Preul MC, Smith KA, et al. *In vivo* intraoperative confocal microscopy for real-time histopathological imaging of brain tumors. *J Neurosurg* 2012;116:854-60.
- Evans CL, Xu X, Kesari S, Xie XS, Wong ST, Young GS. Chemically-selective imaging of brain structures with CARS microscopy. *Opt Express* 2007;15:12076-87.
- Feindel W, Yamamoto YL, Hodge CP. Red cerebral veins and the cerebral steal syndrome. Evidence from fluorescein angiography and microregional blood flow by radioisotopes during excision of an angioma. *J Neurosurg* 1971;35:167-79.
- Floeth FW, Sabel M, Ewelt C, Stummer W, Felsberg J, Reifenberger G, et al. Comparison of (18) F-FET PET and 5-ALA fluorescence in cerebral gliomas. *Eur J Nucl Med Mol Imaging* 2011;38:731-41.
- Foersch S, Heimann A, Ayyad A, Spoden GA, Florin L, Mpoukouvalas K, et al. Confocal laser endomicroscopy for diagnosis and histomorphologic imaging of brain tumors *in vivo*. *PLoS One* 2012;7:e41760.
- Foyer C, Lelandais M, Kunert K. Photooxidative stress in plants. *Physiol Plant* 1994;92:696-717.
- Frangioni JV. *In vivo* near-infrared fluorescence imaging. *Curr Opin Chem Biol* 2003;7:626-34.
- Gioux S, Choi HS, Frangioni JV. Image-guided surgery using invisible near-infrared light: Fundamentals of clinical translation. *Mol Imaging* 2010;9:237-55.
- Goetz M, Deris I, Vieth M, Murr E, Hoffman A, Delaney P, et al. Near-infrared confocal imaging during mini-laparoscopy: A novel rigid endomicroscope with increased imaging plane depth. *J Hepatol* 2010;53:84-90.
- Goetz M, Fottner C, Schirrmacher E, Delaney P, Gregor S, Schneider C, et al. *In vivo* confocal real-time mini-microscopy in animal models of human inflammatory and neoplastic diseases. *Endoscopy* 2007;39:350-6.
- Goetz M, Vieth M, Kanzler S, Galle PR, Delaney P, Neurath MF, et al. *In vivo* confocal laser laparoscopy allows real time subsurface microscopy in animal models of liver disease. *J Hepatol* 2008;48:91-7.
- Gonzalez S, Swindells K, Rajadhyaksha M, Torres A. Changing paradigms in dermatology: Confocal microscopy in clinical and surgical dermatology. *Clin Dermatol* 2003;21:359-69.
- Greish K. Enhanced permeability and retention (EPR) effect and tumor selective delivery of anticancer drugs. London: Imperial College Press; 2006. p. 37-52.
- Gunther U, Epple HJ, Heller F, Loddenkemper C, Grünbaum M, Schneider T, et al. *In vivo* diagnosis of intestinal spirochaetosis by confocal endomicroscopy. *Gut* 2008;57:1331-3.
- Gurfinkel M, Thompson AB, Ralston W, Troy TL, Moore AL, Moore TA, et al. Pharmacokinetics of ICG and HPPH-car for the detection of normal and tumor tissue using fluorescence, near-infrared reflectance imaging: A case study. *Photochem Photobiol* 2000;72:94-102.
- Haglund MM, Berger MS, Hochman DW. Enhanced optical imaging of human gliomas and tumor margins. *Neurosurgery* 1996;38:308-17.
- Hansen DA, Spence AM, Carski T, Berger MS. Indocyanine green (ICG) staining and demarcation of tumor margins in a rat glioma model. *Surg Neurol* 1993;40:451-6.
- Hicks SP, Swindells KJ, Middelkamp-Hup MA, Sifakis MA, González E, González S. Confocal histopathology of irritant contact dermatitis *in vivo* and the impact of skin color (black vs white). *J Am Acad Dermatol* 2003;48:727-34.
- Hirche C, Dresel S, Krempien R, Hünerbein M. Sentinel node biopsy by indocyanine green retention fluorescence detection for inguinal lymph node staging of anal cancer: Preliminary experience. *Ann Surg Oncol* 2010;17:2357-62.
- Hsi RA, Rosenthal DI, Glatstein E. Photodynamic therapy in the treatment of cancer: Current state of the art. *Drugs* 1999;57:725-34.
- Hsiung PL, Hardy J, Friedland S, Soetikno R, Du CB, Wu AP, et al. Detection of colonic dysplasia *in vivo* using a targeted heptapeptide and confocal microendoscopy. *Nat Med* 2008;14:454-8.
- Ishihara R, Katayama Y, Watanabe T, Yoshino A, Fukushima T, Sakatani K. Quantitative spectroscopic analysis of 5-aminolevulinic acid-induced protoporphyrin IX fluorescence intensity in diffusely infiltrating astrocytomas. *Neurol Med Chir (Tokyo)* 2007;47:53-7.
- Iwai K, Maeda H, Konno T. Use of oily contrast medium for selective drug

- targeting to tumor: Enhanced therapeutic effect and X-ray image. *Cancer Res* 1984;44:2115-21.
47. Jabbour JM, Cheng S, Malik BH, Cuenca R, Jo JA, Wright J, et al. Fluorescence lifetime imaging and reflectance confocal microscopy for multiscale imaging of oral precancer. *J Biomed Opt* 2013;18:046012.
  48. Jabbour JM, Saldua MA, Bixler JN, Maitland KC. Confocal endomicroscopy: Instrumentation and medical applications. *Ann Biomed Eng* 2012;40:378-97.
  49. Kelder W, Nimura H, Takahashi N, Mitsumori N, van Dam GM, Yanaga K. Sentinel node mapping with indocyanine green (ICG) and infrared ray detection in early gastric cancer: An accurate method that enables a limited lymphadenectomy. *Eur J Surg Oncol* 2010;36:552-8.
  50. Kennedy JC, Marcus SL, Pottier RH. Photodynamic therapy (PDT) and photodiagnosis (PD) using endogenous photosensitization induced by 5-aminolevulinic acid (ALA): Mechanisms and clinical results. *J Clin Laser Med Surg* 1996;14:289-304.
  51. Kiesslich R, Burg J, Vieth M, Gnaendiger J, Enders M, Delaney P, et al. Confocal laser endoscopy for diagnosing intraepithelial neoplasias and colorectal cancer *in vivo*. *Gastroenterology* 2004;127:706-13.
  52. Klatzo I, Miguel J, Otenasek R. The application of fluorescein labeled serum proteins (FLSP) to the study of vascular permeability in the brain. *Acta Neuropathol (Berl)* 1962;2:144-60.
  53. Koc K, Anik I, Cabuk B, Ceylan S. Fluorescein sodium-guided surgery in glioblastoma multiforme: A prospective evaluation. *Br J Neurosurg* 2008;22:99-103.
  54. Krammer B, Plaetzer K. ALA and its clinical impact, from bench to bedside. *Photochem Photobiol Sci* 2008;7:283-9.
  55. Kuroiwa T, Kajimoto Y, Ohta T. Development of a fluorescein operative microscope for use during malignant glioma surgery: A technical note and preliminary report. *Surg Neurol* 1998;50:41-8.
  56. Lacroix M, bi-Said D, Fournay DR, Gokaslan ZL, Shi W, DeMonte F, et al. A multivariate analysis of 416 patients with glioblastoma multiforme: Prognosis, extent of resection, and survival. *J Neurosurg* 2001;95:190-8.
  57. Laemmel E, Genet M, Le Goualher G, Perchant A, Le Gargasson JF, Vicaut E. Fibered confocal fluorescence microscopy (Cell-viZio) facilitates extended imaging in the field of microcirculation. A comparison with intravital microscopy. *J Vasc Res* 2004;41:400-11.
  58. Lamborn KR, Chang SM, Prados MD. Prognostic factors for survival of patients with glioblastoma: Recursive partitioning analysis. *Neuro Oncol* 2004;6:227-35.
  59. Licha K. Contrast agents for optical imaging. *Top Curr Chem* 2002;222:1-29.
  60. Little JR, Yamamoto YL, Feindel W, Meyer E, Hodge CP. Superficial temporal artery to middle cerebral artery anastomosis. Intraoperative evaluation by fluorescein angiography and xenon-133 clearance. *J Neurosurg* 1979;50:560-9.
  61. Maeda H, Matsumura Y. Tumorotropic and lymphotropic principles of macromolecular drugs. *Crit Rev Ther Drug Carrier Syst* 1989;6:193-210.
  62. Marcu L. Fluorescence lifetime techniques in medical applications. *Ann Biomed Eng* 2012;40:304-31.
  63. Martin RM, Leonhardt H, Cardoso MC. DNA labeling in living cells. *Cytometry A* 2005;67:45-52.
  64. Martirosyan NL, Cavalcanti DD, Eschbacher JM, Delaney PM, Scheck AC, Abdelwahab MG, et al. Use of *in vivo* near-infrared laser confocal endomicroscopy with indocyanine green to detect the boundary of infiltrative tumor. *J Neurosurg* 2011;115:1131-8.
  65. Matsui A, Lee BT, Winer JH, Vooght CS, Laurence RG, Frangioni JV. Real-time intraoperative near-infrared fluorescence angiography for perforator identification and flap design. *Plast Reconstr Surg* 2009;123:125-7e.
  66. Matsui A, Tanaka E, Choi HS, Winer JH, Kianzad V, Gioux S, et al. Real-time intra-operative near-infrared fluorescence identification of the extrahepatic bile ducts using clinically available contrast agents. *Surgery* 2010;148:87-95.
  67. Matsumura Y, Maeda H. A new concept for macromolecular therapeutics in cancer chemotherapy: Mechanism of tumorotropic accumulation of proteins and the antitumor agent smancs. *Cancer Res* 1986;46:6387-92.
  68. Miura Y, Huettmann G, Orzekowsky-Schroeder R, Steven P, Szaszak M, Koop N, et al. Two-photon microscopy and fluorescence lifetime imaging of retinal pigment epithelial cells under oxidative stress. *Invest Ophthalmol Vis Sci* 2013;54:3366-77.
  69. Moore GE, Peyton WT. The clinical use of fluorescein in neurosurgery; the localization of brain tumors. *J Neurosurg* 1948;5:392-8.
  70. Murray KJ. Improved surgical resection of human brain tumors: Part I. A preliminary study. *Surg Neurol* 1982;17:316-9.
  71. Neumann H, Kiesslich R, Wallace MB, Neurath MF. Confocal laser endomicroscopy: Technical advances and clinical applications. *Gastroenterology* 2010;139:388-92, 392.e1-2.
  72. Ogawa M, Kosaka N, Choyke PL, Kobayashi H. *In vivo* molecular imaging of cancer with a quenching near-infrared fluorescent probe using conjugates of monoclonal antibodies and indocyanine green. *Cancer Res* 2009;69:1268-72.
  73. Ohnishi S, Lomnes SJ, Laurence RG, Gogbashian A, Mariani G, Frangioni JV. Organic alternatives to quantum dots for intraoperative near-infrared fluorescent sentinel lymph node mapping. *Mol Imaging* 2005;4:172-81.
  74. Okuda T, Kataoka K, Taneda M. Metastatic brain tumor surgery using fluorescein sodium: Technical note. *Minim Invasive Neurosurg* 2007;50:382-4.
  75. Olsen TW, Lim JJ, Capone AJ, Myles RA, Gilman JA. Anaphylactic shock following indocyanine green angiography. *Arch Ophthalmol* 1996;114:97.
  76. Lakowicz JR. (2006). *Principles of Fluorescence Spectroscopy*. Baltimore, MD, USA: Springer.
  77. Peng Q, Warloe T, Berg K, Moan J, Kongshaug M, Giercksky KE, et al. 5-Aminolevulinic acid-based photodynamic therapy. Clinical research and future challenges. *Cancer* 1997;79:2282-308.
  78. Petrovsky A, Schellenberger E, Josephson L, Weissleder R, Bogdanov A Jr. Near-infrared fluorescent imaging of tumor apoptosis. *Cancer Res* 2003;63:1936-42.
  79. Pogue BW, Gibbs-Strauss S, Valdes PA, Samkoe K, Roberts DW, Paulsen KD. Review of Neurosurgical Fluorescence Imaging Methodologies. *IEEE J Sel Top Quantum Electron* 2010;16:493-505.
  80. Polom K, Murawa D, Rho YS, Nowaczyk P, Hünnerbein M, Murawa P. Current trends and emerging future of indocyanine green usage in surgery and oncology: A literature review. *Cancer* 2011;117:4812-22.
  81. Raabe A, Nakaji P, Beck J, Kim LJ, Hsu FP, Kameron JD, et al. Prospective evaluation of surgical microscope-integrated intraoperative near-infrared indocyanine green videoangiography during aneurysm surgery. *J Neurosurg* 2005;103:982-9.
  82. Rajadhyaksha M, Gonzalez S, Zavislan JM, Anderson RR, Webb RH. *In vivo* confocal scanning laser microscopy of human skin II: Advances in instrumentation and comparison with histology. *J Invest Dermatol* 1999;113:293-303.
  83. Rivera DR, Brown CM, Ouzounov DG, Pavlova I, Kobat D, Webb WW, et al. Compact and flexible raster scanning multiphoton endoscope capable of imaging unstained tissue. *Proc Natl Acad Sci U S A* 2011;108:17598-603.
  84. Sakashita M, Inoue H, Kashida H, Tanaka J, Cho JY, Satodate H, et al. Virtual histology of colorectal lesions using laser-scanning confocal microscopy. *Endoscopy* 2003;35:1033-8.
  85. Sanai N, Berger MS. Glioma extent of resection and its impact on patient outcome. *Neurosurgery* 2008;62:753-64.
  86. Sanai N, Eschbacher J, Hattendorf G, Coons SW, Preul MC, Smith KA, et al. Intraoperative confocal microscopy for brain tumors: A feasibility analysis in humans. *Neurosurgery* 2011;68:282-90.
  87. Sanai N, Snyder LA, Honea NJ, Coons SW, Eschbacher JM, Smith KA, et al. Intraoperative confocal microscopy in the visualization of 5-aminolevulinic acid fluorescence in low-grade gliomas. *J Neurosurg* 2011;115:740-8.
  88. Sankar T, Delaney PM, Ryan RW, Eschbacher J, Abdelwahab M, Nakaji P, et al. Miniaturized handheld confocal microscopy for neurosurgery: Results in an experimental glioblastoma model. *Neurosurgery* 2010;66:410-7.
  89. Schlosser HG, Suess O, Vajkoczy P, van Landeghem FK, Zeitz M, Bojarski C. Confocal neurolasermicroscopy in human brain-perspectives for neurosurgery on a cellular level (including additional comments to this article). *Cent Eur Neurosurg* 2010;71:13-9.
  90. Sharma R, Wang W, Rasmussen JC, Joshi A, Houston JP, Adams KE, et al. Quantitative imaging of lymph function. *Am J Physiol Heart Circ Physiol* 2007;292:H3109-18.
  91. Shi Y, Zhang D, Huff TB, Wang X, Shi R, Xu XM, et al. Longitudinal *in vivo* coherent anti-Stokes Raman scattering imaging of demyelination and remyelination in injured spinal cord. *J Biomed Opt* 2011;16:106012.
  92. Shinoda J, Yano H, Yoshimura S, Okumura A, Kaku Y, Iwama T, et al. Fluorescence-guided resection of glioblastoma multiforme by using high-dose fluorescein sodium. Technical note. *J Neurosurg* 2003;99:597-603.
  93. Skinner SA, Tutton PJ, O'Brien PE. Microvascular architecture of experimental colon tumors in the rat. *Cancer Res* 1990;50:2411-7.
  94. Song L, van Gijlswijk RP, Young IT, Tanke HJ. Influence of fluorochrome labeling density on the photobleaching kinetics of fluorescein in microscopy. *Cytometry* 1997;27:213-23.

95. Song L, Varma CA, Verhoeven JW, Tanke HJ. Influence of the triplet excited state on the photobleaching kinetics of fluorescein in microscopy. *Biophys J* 1996;70:2959-68.
96. Sonn GA, Jones SN, Tarin TV, Du CB, Mach KE, Jensen KC, et al. Optical biopsy of human bladder neoplasia with *in vivo* confocal laser endomicroscopy. *J Urol* 2009;182:1299-305.
97. Stefania S, Simona S, Paola A, Luisa B, Stefania B, Jennifer C, et al. High-resolution multiphoton tomography and fluorescence lifetime imaging of UVB-induced cellular damage on cultured fibroblasts producing fibres. *Skin Res Technol* 2013;19:251-7.
98. Stummer W, Novotny A, Stepp H, Goetz C, Bise K, Reulen HJ. Fluorescence-guided resection of glioblastoma multiforme by using 5-aminolevulinic acid-induced porphyrins: A prospective study in 52 consecutive patients. *J Neurosurg* 2000;93:1003-13.
99. Stummer W, Pichlmeier U, Meinel T, Wiestler OD, Zanella F, Reulen HJ; ALA-Glioma Study Group. Fluorescence-guided surgery with 5-aminolevulinic acid for resection of malignant glioma: A randomised controlled multicentre phase III trial. *Lancet Oncol* 2006;7:392-401.
100. Stummer W, Stepp H, Moller G, Ehrhardt A, Leonhard M, Reulen HJ. Technical principles for protoporphyrin-IX-fluorescence guided microsurgical resection of malignant glioma tissue. *Acta Neurochir (Wien)* 1998;140:995-1000.
101. Stupp R, Hegi ME, Mason WP, van den Bent MJ, Taphoorn MJ, Janzer RC, et al. Effects of radiotherapy with concomitant and adjuvant temozolomide versus radiotherapy alone on survival in glioblastoma in a randomised phase III study: 5-year analysis of the EORTC-NCIC trial. *Lancet Oncol* 2009;10:459-66.
102. Sun Y, Hatami N, Yee M, Phipps J, Elson DS, Gorin F, et al. Fluorescence lifetime imaging microscopy for brain tumor image-guided surgery. *J Biomed Opt* 2010;15:056022.
103. Suzuki M, Hori K, Abe I, Saito S, Sato H. A new approach to cancer chemotherapy: Selective enhancement of tumor blood flow with angiotensin II. *J Natl Cancer Inst* 1981;67:663-9.
104. Tagaya N, Yamazaki R, Nakagawa A, Abe A, Hamada K, Kubota K, et al. Intraoperative identification of sentinel lymph nodes by near-infrared fluorescence imaging in patients with breast cancer. *Am J Surg* 2008;195:850-3.
105. Tan J, Quinn MA, Pyman JM, Delaney PM, McLaren WJ. Detection of cervical intraepithelial neoplasia *in vivo* using confocal endomicroscopy. *BJOG* 2009;116:1663-70.
106. Tanaka E, Chen FY, Flaumenhaft R, Graham GJ, Laurence RG, Frangioni JV. Real-time assessment of cardiac perfusion, coronary angiography, and acute intravascular thrombi using dual-channel near-infrared fluorescence imaging. *J Thorac Cardiovasc Surg* 2009;138:133-40.
107. Tanaka Y, Nariai T, Momose T, Aoyagi M, Maehara T, Tomori T, et al. Glioma surgery using a multimodal navigation system with integrated metabolic images. *J Neurosurg* 2009;110:163-72.
108. Te Velde EA, Veerman T, Subramaniam V, Ruers T. The use of fluorescent dyes and probes in surgical oncology. *Eur J Surg Oncol* 2010;36:6-15.
109. Thiberville L, Moreno-Swirc S, Vercauteren T, Peltier E, Cavé C, Bourg Heckly G. *In vivo* imaging of the bronchial wall microstructure using fibered confocal fluorescence microscopy. *Am J Respir Crit Care Med* 2007;175:22-31.
110. Tilgner J, Herr M, Ostertag C, Volk B. Validation of intraoperative diagnoses using smear preparations from stereotactic brain biopsies: Intraoperative versus final diagnosis--influence of clinical factors. *Neurosurgery* 2005;56:257-65.
111. Tilli MT, Cabrera MC, Parrish AR, Torre KM, Sidawy MK, Gallagher AL, et al. Real-time imaging and characterization of human breast tissue by reflectance confocal microscopy. *J Biomed Opt* 2007;12:051901.
112. Tonn JC, Stummer W. Fluorescence-guided resection of malignant gliomas using 5-aminolevulinic acid: Practical use, risks, and pitfalls. *Clin Neurosurg* 2008;55:20-6.
113. Uematsu Y, Owai Y, Okita R, Tanaka Y, Itakura T. The usefulness and problem of intraoperative rapid diagnosis in surgical neuropathology. *Brain Tumor Pathol* 2007;24:47-52.
114. Ustione A, Piston DW. A simple introduction to multiphoton microscopy. *J Microsc* 2011;243:221-6.
115. Vrouenraets MB, Visser GW, Snow GB, van Dongen GA. Basic principles, applications in oncology and improved selectivity of photodynamic therapy. *Anticancer Res* 2003;23:505-22.
116. Wallace MB, Meining A, Canto MI, Fockens P, Miehlke S, Roesch T, et al. The safety of intravenous fluorescein for confocal laser endomicroscopy in the gastrointestinal tract. *Aliment Pharmacol Ther* 2010;31:548-52.
117. Wallner KE, Galicich JH, Krol G, Arbit E, Malkin MG. Patterns of failure following treatment for glioblastoma multiforme and anaplastic astrocytoma. *Int J Radiat Oncol Biol Phys* 1989;16:1405-9.
118. Wen PY, Kesari S. Malignant gliomas in adults. *N Engl J Med* 2008;359:492-507.
119. White WM, Tearney GJ, Pilch BZ, Fabian RL, Anderson RR, Gaz RD. A novel, noninvasive imaging technique for intraoperative assessment of parathyroid glands: Confocal reflectance microscopy. *Surgery* 2000;128:1088-100.
120. Wiesner C, Jager W, Salzer A, Biesterfeld S, Kiesslich R, Hampel C, et al. Confocal laser endomicroscopy for the diagnosis of urothelial bladder neoplasia: A technology of the future? *BJU Int* 2011;107:399-403.
121. Wright A, Bubb WA, Hawkins CL, Davies MJ. Singlet oxygen-mediated protein oxidation: Evidence for the formation of reactive side chain peroxides on tyrosine residues. *Photochem Photobiol* 2002;76:35-46.
122. Wrobel CJ, Meltzer H, Lamond R, Alksne JF. Intraoperative assessment of aneurysm clip placement by intravenous fluorescein angiography. *Neurosurgery* 1994;35:970-3.
123. Georges J, Zehri A, Carlson E, Nichols J, Mooney MA, Martirosyan NL, et al. Contrast-free microscopic assessment of glioblastoma biopsy specimens prior to biobanking. *Neurosurg Focus* 2014;36:E8.
124. Gao L, Wang Z, Li F, Hammoudi AA, Thrall MJ, Cagle PT, et al. Differential diagnosis of lung carcinoma with coherent anti-Stokes Raman scattering imaging. *Arch Pathol Lab Med* 2012;136:1502-10.
125. Adur J, Pelegati VB, de Thomaz AA, Baratti MO, Almeida DB, Andrade LA, et al. Optical biomarkers of serous and mucinous human ovarian tumor assessed with nonlinear optics microscopies. *PLoS One* 2012;7:e47007.
126. Wu X, Chen G, Lu J, Zhu W, Qiu J, Chen J, et al. Label-free detection of breast masses using multiphoton microscopy. *PLoS One* 2013;8:e65933.